Singularities, Shocks, and Instabilities in Interface Growth

By V. Tsemekhman and J. S. Wettlaufer

Two-dimensional interface motion is examined in the setting of geometric crystal growth. We focus on the relationships between local curvature and global shape evolution displaying the dual role of singularities and shocks depending on the parameterization of the curve—the crystal surface. Discontinuities in surface slope accompany regions of asymptotically decreasing curvature during transient growth, whereas an absence of discontinuities preempts such asymptotic curvature evolution. In one parameterization, these discontinuities manifest themselves as a finite-time continuous blowup of curvature, and in another, as a shock and hence a localized divergence of curvature. Previously, it has been conjectured, based on numerical evidence, that the minimum blowup time is preempted by shock formation. We prove this conjecture in the present paper. Additionally we prove that a class of local geometric models preserves the convexity of the surface. These results are connected to experiments on crystal growth.

1. Background and motivation

The evolution of the interface between two phases or different domains of the same phase exhibits behavior of fundamental importance in condensed matter

Address for correspondence: V. Tsemekhman, Applied Physics Laboratory, University of Washington, Box 355640, Seattle, WA 98105; e-mail: dima@apl.washington.edu. Useful conversations with M. Maruyama, H. Stern, R. LeVeque, and S. Mitran are gratefully acknowledged, as is a critical reading of the manuscript by L. N. Howard. Some of the analysis described here is the outgrowth of a previous collaboration between JSW and M. Jackson. We have benefited greatly from that collaboration. This work has been supported by NSF Grants CHE99-80125 and INT97-25945.

STUDIES IN APPLIED MATHEMATICS 110:221–256

Published by Blackwell Publishing, 350 Main Street, Malden, MA 02148, USA, and 9600 Garsington Road, Oxford, OX4 2DQ, UK.

science while forming a test bed for the mathematics of singularities and shape dynamics. The relationships between interfacial convexity, nonlocality, and singularity formation, among others, all present themselves naturally in the context of crystal growth where we find sound physical constraints to a host of general mathematical developments. Although our primary interest here is to elucidate the process of transient highly anisotropic crystal growth [1, 2], the developments are broadly applicable to the dynamics of interfaces separating two fluids [3, 4], phase-antiphase boundary motion [5], magnetic fluid domains [6], grain growth and Ostwald ripening [7], chemical fronts [8], and vortex motion [9]. Recently, there has been a flurry of activity surrounding the so-called "geometric" crystal growth in which the mathematical approaches hold relevance for many of the physical settings mentioned above. There are two situations that have been studied within a geometric framework: diffusion-limited and interface-controlled growth. In the former, the interfacial motion is controlled by long-ranged diffusional influences such as the removal of latent heat or impurities and in such situations one must invoke a boundary layer hypothesis to work within the geometric framework.[1] In the latter case, the motion of the interface is controlled solely by local interfacial properties and molecular kinetics so that the geometric description is naturally applicable *ab initio*. In this paper, we also discuss a third situation when geometric growth models are applicable, namely, when significant changes in the "shape" of the interface take place on a time scale short compared to characteristic times for bulk diffusion.

A central paradigm in interface-controlled growth is that of the global shape evolution of a partially faceted shape. Qualitatively, this is a crystal that has both slowly growing molecularly smooth faces, known as *facets*, and faces that are molecularly rough and grow much more rapidly. These two types of interface originate because of orientation dependence, relative to the crystallographic lattice, of the bond strength and hence surface energy. The detailed structure of a given face depends on temperature. In equilibrium, above a critical temperature called the thermodynamic roughening temperature, a facet will become molecularly rough. A facet can also become rough during growth because the flux of molecules toward the surface is too large to be accommodated by a

[1] The boundary layer hypothesis posits that the field variable which is being dissipated normal to the growth front (e.g., temperature or impurity concentration) is confined to a narrow region of the parent phase adjacent to the interface, the scale of which depends on the growth rate and the diffusivity of the field, and that this scale is small relative to the characteristic variation parallel to the interface. In the asymptotic limit that the ratio of the above scales is small, geometric models can be appropriate for diffusion limited growth, but in general diffusion limited growth cannot be treated as geometric because the interfacial motion depends on the interfacial value of the field variable(s) which are modified by diffusion. Further complications arise when anisotropy is included. The most common approach is to ascribe an orientation dependence to the surface tension or the kinetic coefficient, or to both. Reference [1] reviews geometric models with the primary focus on solidification. Some papers of note in this regard are included in [10]. The mathematics of interface motion is discussed in [11].

growth mechanism that maintains one crystallographic orientation. Therefore, a partially faceted shape is one for which some interfacial orientations exist at a temperature below their thermodynamic roughening temperature, and the growth drive is weaker than that required for kinetic roughening to be operative at those orientations. Facets appear at crystallographic orientations for which the equilibrium surface free energy is a minimum. Facets coexist with areas of the surface that are covered with regular steps and are therefore rough. Monomolecular height steps, separating terraces of a given orientation, are known to be rough at any temperature due to the finite density of kinks along their edges. The study of partially faceted shapes was initiated by Wulff [12] and developed in the classical kinematic theories of Frank [13][2] and Chernov [16] which first described the dominance on the evolving shape of the slowest growing orientations. Facets present on the initial shape require an activation process to grow in a direction normal to themselves, while under the same growth drive, molecularly rough orientations present the parent phase with no barrier to growth. Qualitatively, therefore, we expect the majority of the surface of an asymptotic growth shape will comprise the slowly growing facets, and this is indeed observed (e.g., [17–19]). However, in most practical situations one observes "transient" growth shapes, therefore an important question concerns the processes which take an initial crystalline seed toward a faceted asymptotic growth shape. Recently, a commonly observed feature of this overall shape transition, or *global kinetic faceting*, has been predicted theoretically [2]. The process centers on the transient evolution of a partially faceted shape toward a fully faceted shape whereby the rough orientations grow out of existence with *decreasing* curvature. Intuitively we can understand that, for a convex shape, the surface slope can remain continuous if one allows curvature to increase, but a decrease in curvature must be accompanied by jumps in the surface slope. A principal goal of our work is to relate the local curvature evolution to the global shape dynamics.

An important part of the edifice of first-order partial differential equations is the mathematics of shock formation. This plays a pivotal role in the setting of crystal growth because the jumps in surface slope accompanying a decrease in interfacial curvature are associated with the formation of shocks in the evolution equation of the surface. Hence several of the most dramatic aspects of transient shape evolution, which wed equilibrium and asymptotic growth shapes, are associated with the formation and evolution of shocks and the blowup of interfacial curvature. An abrupt change in surface slope separates structurally distinct regions of a growing crystal surface; for example, as described above, facets may be flanked by molecularly rough regions. By parity

[2]An extension of this work to three dimensions was presented in [14]. Using Frank's approach J. Villain [15] provides an example where curvature in the slow growth directions decreases.

of reasoning, the absence of shocks, and hence the absence of discontinuities in surface slope, must tell us something about global shape dynamics. Since we are most likely to observe transient growth, shock dynamics are central to the interpretation of experimental data. Measurements of robust features, such as the evolution of interfacial discontinuities, are more accessible experimentally, so that an understanding of how the shock trajectories depend on the physics of the solidification processes makes direct contact with observation [20].

In this paper we prove a previous conjecture, based on numerical evidence, concerning the finite-time curvature divergence of a growing crystal [2]. It was conjectured that the minimum blowup time for the curvature of particular orientations occurs *after* the formation of a shock that limits the surface to discontinuous rather than continuous but singular curvature development. We also show that the origins of shock structure make a direct connection with surface growth and diffusion processes, and hence with experiment. By measuring the curvature evolution one can extract the local growth rate function thereby forming a test bed for theories [20]. The work suggests new experiments and a possible reanalysis of existing experiments on two-dimensional growth [21].[3] The analysis may also be of interest to nonglobal shape evolution such as the partially faceted needle crystal problem [22], and singularity formation in the modified Kuramoto–Sivashinsky equation resulting from the application of the boundary layer hypothesis to diffusion-limited growth [23]. Finally, we prove that the local geometric models wherein the normal growth velocity depends only on the local orientation of the surface preserve the convexity of the surface.

2. Geometric evolution

We study the process of crystal growth under the conditions in which a geometric model describes the motion of the phase boundary. Here, we distinguish between geometric models whereby the local velocity can depend on curvature, i.e., like motion by mean curvature [5], and those wherein the velocity does not depend on curvature [2]. For simplicity, we treat the case of a two-dimensional crystal. Our goal then is to understand the properties of the solutions of the evolution equation

$$\frac{\partial \vec{C}}{\partial t} = -V\vec{N}. \tag{1}$$

Here $\vec{C} = \vec{C}(u, t)$ is an evolving plane curve parameterized by a variable u, $\vec{N}$ is the (inward-pointing) unit normal vector, and V is the normal growth

[3]Examples of two-dimensional growth include, among others, metal [18] and ice [19] crystallite growth, the theory of spiral growth [21] and the crystallization of monolayers of soluble surfactants [21].

velocity. The arclength s and u are related by $s(u,t) = \int_0^u |\partial \vec{C}(u',t)/\partial u'| du'$. As described above, herein we study the case when the growth velocity depends only on the local orientation of the surface normal: $V = V(\theta)$, where θ is an angle between the positive x-axis and the unit tangent vector $\vec{T}$. We expect that the variety of possible functional forms of the growth function $V(\theta)$ will lead to a rich behavior of solutions for Equation (1).

Exact solutions for this type of evolution equation can be expressed in terms of characteristics. Cahn et al. [1, 24] have shown that if V depends only on θ, the normal to the crystal surface is preserved along characteristics, and these characteristics are given by

$$\vec{r}(\theta,t) = \vec{r}_0(\theta) + \vec{\nabla} V(\theta) t. \tag{2}$$

Here, $\vec{r}_0(\theta)$ is the initial curve and $\vec{\nabla} V(\theta)$ is the gradient evaluated at the points on the surface with normal θ; it is not a surface gradient. We can think of $\vec{\nabla} V(\theta)$ as the name of vector-valued function which depends on $V(\theta)$.

A more useful form of Equation (2) is obtained by parameterizing $\vec{C}$ by θ instead of u. This implies that we are using the same set of variables as in Equation (2). It is clear that such a transformation of variables can be performed as long as there is a one-to-one correspondence between θ and u . It is therefore valid globally as long as the surface is convex, continuous, and does not contain any corners. If corners form, the transformation is valid piecewise between them. It is not applicable, however, at the facets which have to be treated separately. Since $(\partial/\partial t)_\theta = (\partial/\partial t)_u - (\partial\theta/\partial t)_u \partial/\partial\theta$, i.e., time evolution at fixed normal, and $\partial \vec{C}(\theta,t)/\partial\theta = (\partial \vec{C}(\theta,t)/\partial s)/(\partial\theta/\partial s) = 1/\kappa(\theta,t)\vec{T}$, we obtain

$$\left(\frac{\partial \vec{C}(\theta,t)}{\partial t}\right)_\theta = -V(\theta)\vec{N} - \frac{1}{\kappa(\theta,t)}\frac{\partial\theta}{\partial t}. \tag{3}$$

Here $\kappa(\theta,t) = \partial\theta/\partial s$ is the curvature at the location with orientation θ of the normal at time t. Next, in analogy with the approach of Gage and Hamilton [25], as outlined in [2], we write

$$\left(\frac{\partial\theta}{\partial t}\right)_u = -\frac{\partial V}{\partial s}, \tag{4}$$

and using $\partial V/\partial s = \kappa(\theta,t)\partial V/\partial\theta$ we get the final form of the evolution equation for the boundary parameterized by θ:

$$\left(\frac{\partial \vec{C}(\theta,t)}{\partial t}\right)_\theta = -V(\theta)\vec{N} + \frac{dV}{d\theta}\vec{T}. \tag{5}$$

Note that when parameterized by θ, the solution $\vec{C}(\theta,t)$ of the evolution equation (5) describes the trajectory of a point on the surface with a given orientation of the normal θ. Therefore, $\vec{C}(\theta,t)$ is just the characteristic $\vec{r}(\theta,t)$

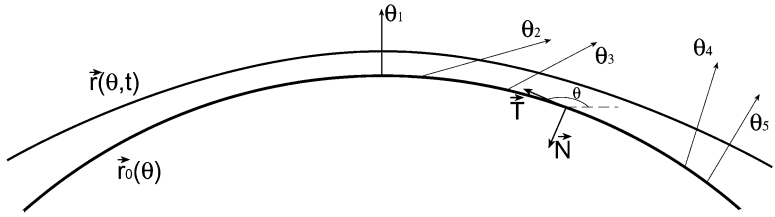

Figure 1. Characteristics for the evolution equation. Each is marked by the orientation of the normal θ that is fixed along the characteristic which represents a ray emanating from the point on the initial curve with orientation θ.

for orientation θ. From this point on we will only be working with a curve parameterized by θ, and all time derivatives will be taken at constant θ. It is convenient then to change the notation: $\vec{r}(\theta, t) \equiv \vec{C}(\theta, t)$, $\partial/\partial t \equiv (\partial/\partial t)_\theta$, and $V'(\theta) \equiv dV/d\theta$. Since the right-hand side of Equation (5) does not depend on time, the solution of this equation can be written in the following form:

$$\vec{r}(\theta, t) = \vec{r}_0(\theta) + (-V(\theta)\vec{N} + V'(\theta)\vec{T})t. \tag{6}$$

Characteristics defined by Equation (6) represent the straight rays starting at the boundary of the seed crystal (Figure 1). The crystal shape at time t is the locus of all points $\vec{r}(t)$ on all characteristics emanating from initial points $\vec{r}_0$, as long as these characteristics do not intersect [1].

Growing shapes resulting from Equation (1) have been analyzed in detail [1, 2, 24] for various functional forms of the growth function $V(\theta)$. The analysis in [2] predicted that for a general class of $V(\theta)$ the growth shape contains areas of decreasing curvature both at the roughest and vicinal orientations—surface areas adjacent to the facet where the density of steps is low. The region between these flattening areas grows with increasing curvature and develops a corner that eventually absorbs all rough orientations. The prediction has since been confirmed by experiment [20]. On the other hand, the expansion of facets, the formation of dynamic facets at rough orientations, and the development of concavities on the initially convex surface are also observed, and hence call for a general study of the geometric model for all possible forms of $V(\theta)$ and the stability of its solutions. We start with the analysis of the development of a shock.

3. Shock propagation and evolution of curvature

3.1. Shock trajectory

When two characteristics intersect, a shock is initiated. It propagates as long as the pairs of intersecting characteristics continue to exist. The location of the intersection point as a function of time determines the shock trajectory.

Intersecting characteristics terminate at the point of intersection. Since in the case of geometric evolution, characteristics represent the trajectories of locations with fixed orientation of the surface normal, their termination implies a disappearance of the corresponding orientations. Therefore, the initiation and propagation of shocks on a crystal surface manifest themselves as the formation and sharpening of a corner.

The jump condition at a shock is determined from the physics of the problem which requires that the crystal surface be continuous, and that, during growth, once the point is within the crystal it stays there [24]. It follows that a shock forms when two characteristics arrive at the same point at the same time. An alternative way to derive this jump condition is from an integral conservation law. The specific case that we deal with here is one of cubic symmetry, and hence, if s_1 and s_2 are the arclengths at the points with $\theta = 0$ and $\theta = \pi/4$, respectively, the conservation law states that the integral $\int_{s_1}^{s_2} \kappa ds$ equals $\pi/4$ at any time [26], and such a law can be generalized for any symmetry.

To obtain the shock trajectory, we now derive the differential equations for the functions that determine members of the intersecting pairs of characteristics at each moment of time. Each member of an intersecting pair of characteristics corresponds to a certain orientation; we denote the two orientations corresponding to a generic intersecting pair by θ_1 and θ_2. Let t_0 be the time when a shock is initiated. We now think of θ_1 and θ_2 as functions of time defined by the following: for each value of $t > t_0$, let θ_1 and θ_2 be the orientations for which the corresponding characteristics intersect at time t.

With these assumptions, we write the intersection of characteristics as [24]

$$\vec{r}(\theta_1(t), t) = \vec{r}(\theta_2(t), t). \tag{7}$$

Differentiating both sides with respect to t gives us

$$\frac{\partial \vec{r}(\theta_1, t)}{\partial \theta_1}\frac{d\theta_1}{dt} + \frac{\partial \vec{r}(\theta_1, t)}{\partial t} = \frac{\partial \vec{r}(\theta_2, t)}{\partial \theta_2}\frac{d\theta_2}{dt} + \frac{\partial \vec{r}(\theta_2, t)}{\partial t}. \tag{8}$$

We can use Equation (6) to write $\partial \vec{r}(\theta_i, t)/\partial \theta_i, i = 1, 2$, as

$$\frac{\partial \vec{r}(\theta_i, t)}{\partial \theta_i} = \frac{\partial \vec{r}_0(\theta_i)}{\partial \theta_i} + \frac{\partial}{\partial \theta_i}(-V(\theta_i)\vec{N}_i + V'(\theta_i)\vec{T}_i)t \tag{9}$$

and $\partial \vec{r}(\theta_i, t)/\partial t$ as

$$\frac{\partial \vec{r}(\theta_i, t)}{\partial t} = (-V(\theta_i)\vec{N}_i + V'(\theta_i)\vec{T}_i). \tag{10}$$

We note that

$$\frac{\partial \vec{r}_0(\theta_i)}{\partial \theta_i} = \frac{1}{\kappa_0(\theta_i)}\vec{T}_i \tag{11}$$

and

$$\frac{\partial}{\partial\theta_i}(-V(\theta_i)\vec{N}_i + V'(\theta_i)\vec{T}_i) = \kappa_0(\theta_i)\tilde{V}(\theta_i)\vec{T}_i, \tag{12}$$

where $\kappa_0(\theta_i)$ is the curvature of the initial seed crystal boundary at the location where normal to the boundary has orientation θ_i, and $\tilde{V} = V + V''$. In the derivation of the last two equations we used the fact that $\partial/\partial\theta = (1/\kappa)\partial/\partial s$, $\partial\vec{r}/\partial s = \vec{T}$, and the Frenet equations

$$\frac{\partial\vec{T}}{\partial\theta} = \vec{N},$$
$$\frac{\partial\vec{N}}{\partial\theta} = -\vec{T}. \tag{13}$$

Finally, applying Equations (9)–(13) to Equation (8) we obtain a system of ordinary differential equations for $\theta_1(t)$ and $\theta_2(t)$:

$$\frac{1}{\kappa_0(\theta_1)}\frac{d\theta_1}{dt}(1 + \tilde{V}_1\kappa_0(\theta_1)t)\vec{T}_1 - \frac{1}{\kappa_0(\theta_2)}\frac{d\theta_2}{dt}(1 + \tilde{V}_2\kappa_0(\theta_2)t)\vec{T}_2$$
$$= \frac{1}{t}(\vec{r}_0(\theta_1) - \vec{r}_0(\theta_2)). \tag{14}$$

We now need to specify the initial conditions. It is clear that if the shape of the initial seed does not contain any corners, so that initially all orientations of the normal are present on the boundary, such a situation persists until a shock is initiated, i.e., for $t \le t_0$. Continuity considerations imply that the elimination of orientations starts with the termination of a single orientation θ_0. In other words, two characteristics intersecting at $t = t_0$ have to correspond to two orientations infinitesimally close to each other. Hence, the angle $\theta_1(t_0)$ necessarily coincides with $\theta_2(t_0)$, and both of them are equal to θ_0. At later times, the functions $\theta_1(t)$ and $\theta_2(t)$ diverge from each other, one taking values smaller than θ_0, the other, greater than θ_0. Then

$$\theta_1|_{t=t_0} = \theta_0,$$
$$\left.\frac{d\theta_1}{dt}\right|_{t=t_0} > 0 \tag{15}$$

and

$$\theta_2|_{t=t_0} = \theta_0,$$
$$\left.\frac{d\theta_2}{dt}\right|_{t=t_0} < 0. \tag{16}$$

Returning to Equation (14) we notice that at $t = t_0$, $\kappa_0(\theta_1) = \kappa_0(\theta_2) \equiv \kappa_0$, $\vec{r}_0(\theta_1) = \vec{r}_0(\theta_2)$, and $\vec{T}_1 = \vec{T}_2$. Hence, at t_0

$$\left.\frac{d\theta_1}{dt}\right|_{t=t_0}(1+\tilde{V}(\theta_0)\kappa_0 t_0) = \left.\frac{d\theta_2}{dt}\right|_{t=t_0}(1+\tilde{V}(\theta_0)\kappa_0 t_0), \tag{17}$$

which, because of Equations (15) and (16), can only be satisfied if

$$t_0 = -\frac{1}{\tilde{V}(\theta_0)\kappa_0}. \tag{18}$$

We immediately conclude from Equation (18) that a shock forms if, for some range of the orientation of the normal θ, $\tilde{V}(\theta) < 0$ [2]. The first orientation that will be eliminated is the one for which t_0 is minimum. It follows that this shock is initiated at the orientation θ_0 such that $\tilde{V}(\theta_0)$ is a global minimum. Equation (18) then allows us to find the time when the shock forms. The physical meaning of Equation (18) will become clear in the next section where we derive the equation for the evolution of curvature.

3.2. Curvature evolution

The convenience of the reparameterization of Equation (1) by variables (θ, t) is reemphasized when deriving the equation for the local evolution of curvature. When curvature is parameterized by $\kappa = \kappa(u, t)$, the curvature evolution equation is nonlocal. However, it has been shown [25] that a parameterization by θ via $\kappa = \kappa(\theta, t)$ yields a simple local evolution equation

$$\frac{\partial \kappa}{\partial t} = -\tilde{V}(\theta)\kappa^2. \tag{19}$$

Equation (19) describes the evolution of the curvature along the trajectory of the location on the boundary with a fixed orientation of the normal θ. The derivation of this equation relies on the fact that the growth function V depends only on θ and is based on the same approach of Gage and Hamilton [25] and is outlined in [2]. Equation (19) is valid as long as the transformation of variables can be performed. The solution of Equation (19) is given by

$$\kappa(\theta, t) = \frac{\kappa_0(\theta)}{1+\tilde{V}(\theta)\kappa_0(\theta)t}, \tag{20}$$

where $\kappa_0(\theta)$ is the curvature at the location on the initial seed crystal's boundary with orientation θ of the normal.

Any seed crystal relevant to our analysis is convex, $\kappa_0(\theta) \geq 0$, but need not be strictly convex, $\kappa_0(\theta) > 0$, since facets can be present on the initial shape. We first treat the evolution of the nonsingular orientations, and return to the discussion of the effects of the facets in Section 4. In [2], the conclusion was made that orientations with $\tilde{V} > 0$ evolve with decreasing curvature. On the other hand, for any orientation with $\tilde{V}(\theta) < 0$ the solution in Equation (20) gives a finite-time curvature divergence at time $t = -(\kappa_0 \tilde{V}(\theta))^{-1}$. The minimum "blowup" time corresponds to the orientation for which $\tilde{V}$ is minimum.

Comparing this result with Equation (18) we conclude that the shock forms exactly at the same orientation and time as the initial curvature divergence.

However, according to Equation (20) the curvature diverges not only for θ_0, but for all θ with negative $\tilde{V}$. Using numerical evidence, it was previously conjectured that characteristics for orientations with $\tilde{V} < 0$ hit the shock before the blowup time, given by Equation (18) [2]. Below we prove this conjecture using an approach outlined previously [27] and the results of the previous sections.

3.3. Elimination of curvature divergence by shock formation

Because it appears that the formation of any corner is accompanied by the divergence of curvature, a natural question arises: What is the difference between the limiting process of curvature divergence and corner expansion via shock propagation? In fact, the two processes are distinctly different. We understand that the curvature evolution described by Equation (19) is a continuous process. At any given time curvature within a small vicinity $\delta\theta$ of the blowup angle grows as $\kappa \sim 1/\delta\theta$. Similarly, for any given angle the curvature behaves as $\kappa \sim 1/\delta t$ within a small enough period of time δt before the corresponding blowup time. Because $\delta\theta$ and δt exist for every time and every angle, respectively, Equation (19) describes a continuous limiting process.

On the contrary, in the case of shock propagation, orientations of the normal change smoothly on each side of the shock but jump at $\theta = \theta_{\text{shock}}$. The curvature does not diverge everywhere, only at the single point where the surface meets the shock and hence, κ has a well-defined finite limit on either side of the shock. However, the limits are different on either side of the shock: $\kappa(\theta^-_{\text{shock}}) \neq \kappa(\theta^+_{\text{shock}})$. Since the normal jumps discontinuously at θ_{shock}, curvature is simply described by a delta-function at $\theta = \theta_{\text{shock}}$, but it is well-defined and finite everywhere else.

The conclusion that the intersection of characteristics always precedes the divergence of the curvature implies that corner formation, as a continuous limiting process signified by the divergence of curvature, never takes place. It is replaced by corner formation due to shock propagation.

First, we show that the orientations immediately adjacent to θ_0, where a shock is initiated and the curvature blows up for the first time, are absorbed by the shock before the curvature at these orientations diverges. Assume that the curvature blowup time t_b for an orientation $\theta_2 = \theta_0 - \delta\theta$, infinitesimally smaller than θ_0, is smaller than the time t_2 when the characteristic for this orientation hits the shock. Since from Equation (20), $1 + \tilde{V}_2\kappa_0(\theta_2)t_b = 0$ for $\tilde{V}_2 < 0$ and $t_2 > t_b$, we conclude that $1 + \tilde{V}_2\kappa_0(\theta_2)t_2 < 0$. According to the initial conditions, $d\theta_2/dt|_{t=t_0} < 0$, and hence at time t_2, we can write Equation (14) in the form

$$\vec{r}_0(\theta_1) - \vec{r}_0(\theta_2) = a\vec{T}_1 + b\vec{T}_2, \tag{21}$$

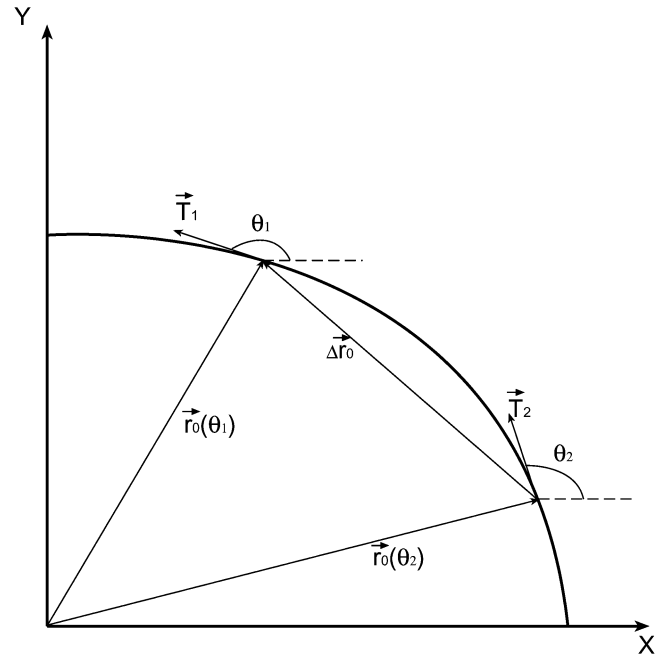

Figure 2. A convex shape and two orientations on it. Since the shape is convex, $\Delta\vec{r}_0$ can only be represented as a linear combination $a\vec{T}_1 + b\vec{T}_2$ if both a and b are positive. Additionally, $\Delta\vec{r}_0$ is never collinear with either $\vec{T}_1$ or $\vec{T}_2$.

where $\vec{T}_1$ corresponds to the orientation θ_1 whose characteristic hits the shock at the same time t_2 as the characteristic with θ_2 does. Here the coefficient b is

$$b = -\frac{1}{\kappa_0(\theta_2)} \left.\frac{d\theta_2}{dt}\right|_{t=t_2} (1 + \tilde{V}_2 \kappa_0(\theta_2) t_2) < 0, \tag{22}$$

and a has a similar form in terms of θ_1.

The crystals we are interested in have at least four-fold symmetry. Hence, we may restrict our study to orientations such that $|\theta_1(t) - \theta_2(t)| < \pi/2$. Then, it is clear from Figure 2 that for a convex initial curve, the vector $\vec{r}_0(\theta_1) - \vec{r}_0(\theta_2)$, described by Equation (21), can only be represented as a linear combination of vectors $\vec{T}_1$ and $\vec{T}_2$ if both a and b are positive. Thus, the assumption $t_b < t_2$ leads us to a contradiction, because $b < 0$. Analogously, this contradiction would have arisen if we had assumed that the blowup time for an orientation θ_1, slightly larger than θ_0, is smaller than the shock intersection time. Hence, immediately after the initiation of the shock the characteristics continue to hit the shock before any possible blowup of curvature.

Now assume that the curvature blowup occurs some finite time Δt after the initiation of the shock. Since at earlier times, the termination of any characteristic at the shock preceded the divergence of curvature along that characteristic, for

a curvature blowup to occur we expect that at $t_0 + \Delta t$ the shock intersection time and the blowup time become equal for some orientation θ_c. Without loss of generality, except that we are restricted to $|\theta_1 - \theta_2| < \pi/2$, we assume that $\theta_c > \theta_0$. Then, since the characteristic with θ_c hits the shock at time $t_0 + \Delta t$, $\theta_c = \theta_1(t_0 + \Delta t)$. Additionally, since the curvature blowup for θ_c takes place at $t_0 + \Delta t$, $1 + \tilde{V}_c \kappa_c^{(0)}(t + \Delta t) = 0$. Then, the first term in Equation (14), taken at time $t + \Delta t$, vanishes and

$$b\vec{T}_2 = \frac{1}{t}(\vec{r}_0(\theta_1) - \vec{r}_0(\theta_2)). \tag{23}$$

If the initial shape is convex, vectors $\vec{T}_2$ and $\vec{r}_0(\theta_1) - \vec{r}_0(\theta_2)$ are never collinear (see Figure 2), and hence, Equation (23) has no solutions. Therefore, every characteristic crosses the shock prior to the time when it joins the continuous limiting process accompanied by the divergence of curvature. In other words, it is shock propagation that is responsible for the disappearance of any orientation.

3.4. Algebraic equation for shock trajectory

The formation of shocks on the surface of an evolving crystal signifies the loss of crystallographic orientations. The subsequent evolution of the shock itself is controlled by the kinetic processes embodied in $V(\theta)$ and hence we now turn our attention to understanding the trajectory of shocks. To that end we derive an algebraic equation that solves Equation (14), and hence determines the members of the pairs of intersecting characteristics. We then use this solution to analyze growth shapes in the presence of facets.

The derivation of the algebraic equation will be based on geometric arguments. It can be misleading to plot characteristics in the plane of the curve with the goal of finding intersecting pairs because many of them intersect in the plane. However, in most cases two orientations arrive at the intersection point at different times, and it is not clear how to discriminate those that form a true intersecting pair on a two-dimensional figure. Therefore, let us consider the evolution of the interface in the three-dimensional space: (x, y, ct) as shown in Figure 3(a). Consider the quantity $c = R/[t]$, which has the units of velocity, wherein R is the length scale and $[t]$ is the time. It is convenient to think of R as the radius of curvature at some location on the boundary of the seed crystal. In the following, we measure the interface velocity in units of c, and use the same notation $V(\theta)$ for dimensionless quantity $V(\theta)/c$. We also render $r_0(\theta)$ dimensionless via $r_0(\theta)/R$. The final result should not depend on R or c. At time t, the point on the interface where the normal $\vec{N}$ makes angle $\theta + \pi/2$ with the x-axis is determined by Equation (6):

$$\vec{r}(\theta, t) = \vec{r}_0(\theta) + (-V(\theta)\vec{N} + V'(\theta)\vec{T})t. \tag{24}$$

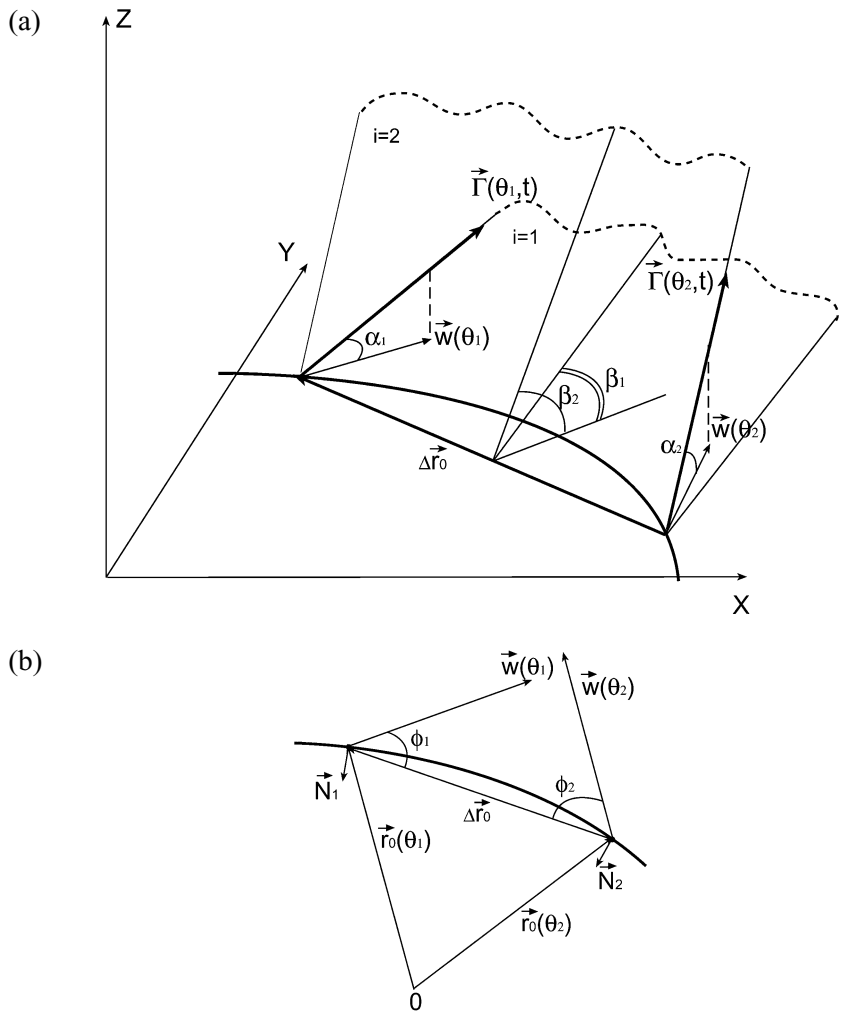

Figure 3. The notation used in the derivation of the algebraic equation (39). (a) Two-dimensional shape evolution in a three-dimensional space. The Z-axis explicitly shows the time coordinate, and the velocity along the characteristic is denoted $\vec{w}(\theta)$. Two characteristics θ_1 and θ_2 intersect if and when the corresponding rays $\vec{\Gamma}(\theta_1, t)$ and $\vec{\Gamma}(\theta_2, t)$ intersect. We denote α_i as an angle between a ray $\vec{\Gamma}(\theta_i, t)$ and a corresponding velocity $\vec{w}(\theta_i)$. Each ray together with a vector $\Delta\vec{r}_0$ forms a plane. We denote β_i as an angle between such a plane and the horizontal plane $Z = 0$. (b) A pair of intersecting characteristics. We denote ϕ_i as an angle between the velocity $\vec{w}(\theta_i)$ and the vector $\Delta\vec{r}_0$.

Let $\vec{w}$ be the velocity along the characteristic which we can write as

$$\vec{w} = -V(\theta)\vec{N} + V'(\theta)\vec{T}. \tag{25}$$

In the three-dimensional space defined above the trajectory of a point on the curve with a fixed orientation θ can be represented with a ray emerging from $\vec{r}_0(\theta)$:

$$\vec{\Gamma}(\theta) = \vec{r}_0(\theta) + t\vec{w} + t\hat{z}. \tag{26}$$

The ray forms an angle α with the (x, y) plane, such that $\tan\alpha = 1/|\vec{w}|$.

Let us now consider a pair of characteristics, θ_1 and θ_2. We form a vector $\Delta\vec{r}_0 = \vec{r}_0(\theta_1) - \vec{r}_0(\theta_2)$ by connecting the starting points of two characteristics. Since $\Delta\vec{r}_0$ and $\vec{\Gamma}(\theta_i)$, $i = 1, 2$, are never collinear (the former does not have a z-component), each such pair of vectors uniquely defines a plane. In general, two different planes are constructed for $i = 1$ and $i = 2$. Since the vector $\Delta\vec{r}_0$ belongs to both of these planes, they necessarily intersect. The case when two planes coincide corresponds to the situation when characteristics θ_1 and θ_2 intersect at some time t. In order for two planes to coincide, they must also form the same angle with the horizontal plane $z = 0$.

Clearly, this is a prescription for solving Equation (14). First, we find an expression for an angle between the constructed and the horizontal planes. Next, we write down an algebraic equation based on the condition that the planes constructed using two different characteristics form the same angle with the horizontal plane. Then, we pick any characteristic θ_1 on either side of the initial value θ_0, and solve the above equation to find the other characteristic θ_2 defining the pair. Finally, to find the time of the intersection, we simply solve a linear equation $\vec{r}(\theta_1, t) = \vec{r}(\theta_2, t)$ that we already know has a solution. Since we should be able to carry out the above steps for any angle θ_1, we will therefore construct a complete solution of Equation (14).

Following the above prescription, let us pick a characteristic corresponding to the orientation $\theta_1 > \theta_0$ and find the angle $\theta_2 > \theta_0$ whose characteristic intersects the one at θ_1 (Figure 3(b)). The result will take the simplest form for an initial crystal shape that is circular. Then $r_0(\theta) = 1$, and it is possible to prove that

$$w_1 \sin\phi_1 = \left| V_1 \cos\frac{\theta_1 - \theta_2}{2} - V_1' \sin\frac{\theta_1 - \theta_2}{2} \right|, \tag{27}$$

and

$$w_2 \sin\phi_2 = \left| V_2 \cos\frac{\theta_1 - \theta_2}{2} + V_2' \sin\frac{\theta_1 - \theta_2}{2} \right|, \tag{28}$$

where ϕ_i, $i = 1, 2$, is the angle between the vectors $\vec{w}_i$ and $\Delta\vec{r}_0$.

Proof: Since the initial shape is a circle with radius 1, $\vec{r}_0(\theta) = -\vec{N}$, and

$$\Delta\vec{r}_0 = \vec{N}_2 - \vec{N}_1. \tag{29}$$

Using the definition (Equation (25)) of $\vec{w}$ we obtain

$$\begin{aligned}\vec{w}_1 \cdot \Delta\vec{r}_0 &= (-V_1\vec{N}_1 + V_1'\vec{T}_1)\cdot(\vec{N}_2 - \vec{N}_1)\\ &= V_1 - V_1(\vec{N}_1\cdot\vec{N}_2) + V_1'(\vec{T}_1\cdot\vec{N}_2)\\ &= V_1\,(1-\cos(\theta_1-\theta_2)) + V_1'\sin(\theta_1-\theta_2)\\ &= 2V_1\sin^2\frac{\theta_1-\theta_2}{2} + V_1'\sin(\theta_1-\theta_2),\end{aligned} \tag{30}$$

and

$$\begin{aligned}\vec{w}_2 \cdot \Delta\vec{r}_0 &= (-V_2\vec{N}_2 + V_2'\vec{T}_2)\cdot(\vec{N}_2 - \vec{N}_1)\\ &= -V_2 + V_2(\vec{N}_1\cdot\vec{N}_2) - V_2'(\vec{T}_2\cdot\vec{N}_1)\\ &= -V_2\,(1-\cos(\theta_1-\theta_2)) + V_2'\sin(\theta_1-\theta_2)\\ &= -2V_2\sin^2\frac{\theta_1-\theta_2}{2} + V_2'\sin(\theta_1-\theta_2).\end{aligned} \tag{31}$$

Therefore, we have

$$\begin{aligned}w_1\cos\phi_1 &= \frac{\vec{w}_1\cdot\Delta\vec{r}_0}{|\Delta\vec{r}_0|}\\ &= \frac{2V_1\sin^2\frac{\theta_1-\theta_2}{2} + V_1'\sin(\theta_1-\theta_2)}{2\sin\frac{\theta_1-\theta_2}{2}}\\ &= V_1\sin\frac{\theta_1-\theta_2}{2} + V_1'\cos\frac{\theta_1-\theta_2}{2},\end{aligned} \tag{32}$$

and

$$\begin{aligned}w_2\cos\phi_2 &= \frac{\vec{w}_2\cdot\Delta\vec{r}_0}{|\Delta\vec{r}_0|}\\ &= \frac{-2V_2\sin^2\frac{\theta_1-\theta_2}{2} + V_2'\sin(\theta_1-\theta_2)}{2\sin\frac{\theta_1-\theta_2}{2}}\\ &= -V_2\sin\frac{\theta_1-\theta_2}{2} + V_2'\cos\frac{\theta_1-\theta_2}{2},\end{aligned} \tag{33}$$

which finally lead to

$$\begin{aligned}w_1^2\sin^2\phi_1 &= w_1^2 - w_1^2\cos^2\phi_1\\ &= \left(V_1^2 + V_1'^2\right) - \left(V_1\sin\frac{\theta_1-\theta_2}{2} + V_1'\cos\frac{\theta_1-\theta_2}{2}\right)^2\\ &= \left(V_1\cos\frac{\theta_1-\theta_2}{2} - V_1'\sin\frac{\theta_1-\theta_2}{2}\right)^2,\end{aligned} \tag{34}$$

and

$$w_2^2 \sin^2 \phi_2 = w_2^2 - w_2^2 \cos^2 \phi_2$$
$$= \left(V_2^2 + V_2'^2\right) - \left(-V_2 \sin \frac{\theta_1 - \theta_2}{2} + V_2' \cos \frac{\theta_1 - \theta_2}{2}\right)^2$$
$$= \left(V_2 \cos \frac{\theta_1 - \theta_2}{2} + V_2' \sin \frac{\theta_1 - \theta_2}{2}\right)^2, \tag{35}$$

proving Equations (27) and (28). ■

As described above, for the two characteristics associated with θ_1 and θ_2 to intersect, the two planes, one formed by vectors $\vec{\Gamma}(\theta_1)$ and $\Delta\vec{r}_0$, the other formed by $\vec{\Gamma}(\theta_2)$ and $\Delta\vec{r}_0$, must coincide. Let ϕ be the angle between $\vec{w}(\theta)$ and the corresponding $\Delta\vec{r}_0$. It is straightforward to show that the angle β between the horizontal plane and the plane formed by two vectors $\vec{\Gamma}(\theta)$ and $\Delta\vec{r}_0$ is determined by

$$\cos \beta = \frac{w(\theta) \sin \phi}{\sqrt{1 + w^2(\theta) \sin^2 \phi}}. \tag{36}$$

The condition that the above two planes coincide can be put in mathematical form by requiring that the angles β_1 and β_2 defined in Equation (36) be equal. Now, in Equation (36) the right-hand side is a monotonically increasing function of the positive variable $u = w \sin \phi$. Therefore, the equation

$$\cos \beta_1 = \cos \beta_2 \tag{37}$$

determining pairs of intersecting characteristics is equivalent to the equation

$$w_1 \sin \phi_1 = w_2 \sin \phi_2. \tag{38}$$

Using (27) and Equation (28), we obtain the following condition:

$$\left| V_1 \cos \frac{\Delta\theta}{2} - V_1' \sin \frac{\Delta\theta}{2} \right| = \left| V_2 \cos \frac{\Delta\theta}{2} + V_2' \sin \frac{\Delta\theta}{2} \right|, \tag{39}$$

where $\Delta\theta = \theta_1 - \theta_2$, thereby providing the final form of the transcendental equation that needs to be solved to determine the pairs of intersecting characteristics.

4. Preservation of convexity in geometric growth

Having studied the general properties of the solutions of Equation (1) we now turn our attention to the growth shapes of the crystals it describes. In particular, we show that for any convex initial crystal shape, which may contain

facets and corners, and any form of the growth function $V(\theta)$, including a nondifferentiable form, the convexity of the boundary is preserved. We start with such growth conditions that either leave the interface completely rough, without any facets, or lead to growth shapes that may contain corners and facets, which are, however, separated from each other by vicinal surfaces. In the next two sections we prove the preservation of convexity for the case when a jump in the orientation of the surface normal develops at the edge of the facet in the process of growth. We also show that in some cases such a geometric model is applicable to the earlier stages of surface evolution while a more elaborate study of the physical processes on the crystal surface may be needed to describe the later stages of crystal growth.

Again, for simplicity but without loss of generality, we study crystals with four-fold symmetry with principal plane orientations at $\theta = n\pi/2$ and the orientations with the highest step density at $\theta = \pi/4 + n\pi/2$. Unless mentioned otherwise, we consider a part of the boundary where $0 \leq \theta \leq \pi/4$. Due to symmetry, all other parts of the crystal boundary evolve identically.

We first notice that in the case of a differentiable $V(\theta)$ and a nonsingular convex initial curve (no facets and no corners) a convexity-preserving solution for Equation (1) exists for all time $t > 0$. For any orientation with $\tilde{V}(\theta) > 0$, Equation (20) predicts that the curvature always stays positive, and the corresponding parts of the boundary remain convex. If $\tilde{V}(\theta) < 0$ for some range of θ, the entire curve remains convex until the minimum blowup time t_0. After the initiation of a shock, at $t > t_0$ the growth shape is defined by two branches separated by a corner where a jump in the orientation of the normal takes place (Figure 4(a)). The two branches are still described by Equations (6) and (20), and hence they retain convexity; the curvature at all surviving orientations remains finite and positive since the divergence of curvature is always preempted by the propagation of a shock. First, orientations with $\tilde{V}(\theta) < 0$ are absorbed by the shock. Until all of them disappear, orientations adjacent to the propagating corner evolve with increasing curvature while the rest of the boundary, including the roughest orientations, grows with decreasing curvature. After all the orientations with $\tilde{V}(\theta) < 0$ have been eliminated, the curvature decreases along the whole boundary. The position of the corner and the jump in the orientation of the normal are determined by the trajectory of the shock. The latter can be expressed in terms of two continuous functions $\theta_1(t)$ and $\theta_2(t)$, which satisfy Equation (14) subject to constraints $\theta_2(t) > 0$ and $\theta_1(t) < \pi/4$.

If at some time $t = t_c$, $\theta_1(t_c) = \pi/4$ while $\theta_2(t_c) = \theta_c^{(2)} > 0$, then all rough orientations leading to $\theta = \pi/4$ disappear, having been absorbed by the shock, while some vicinal orientations leading up to the principal plane orientation $0 < \theta < \theta_c^{(2)}$ continue to grow. At $t = t_c$ the shock propagating on the one side of the symmetry orientation $\theta = \pi/4$ collides with that on the other side (Figure 4(b)). A secondary shock develops that, due to symmetry of the crystal,

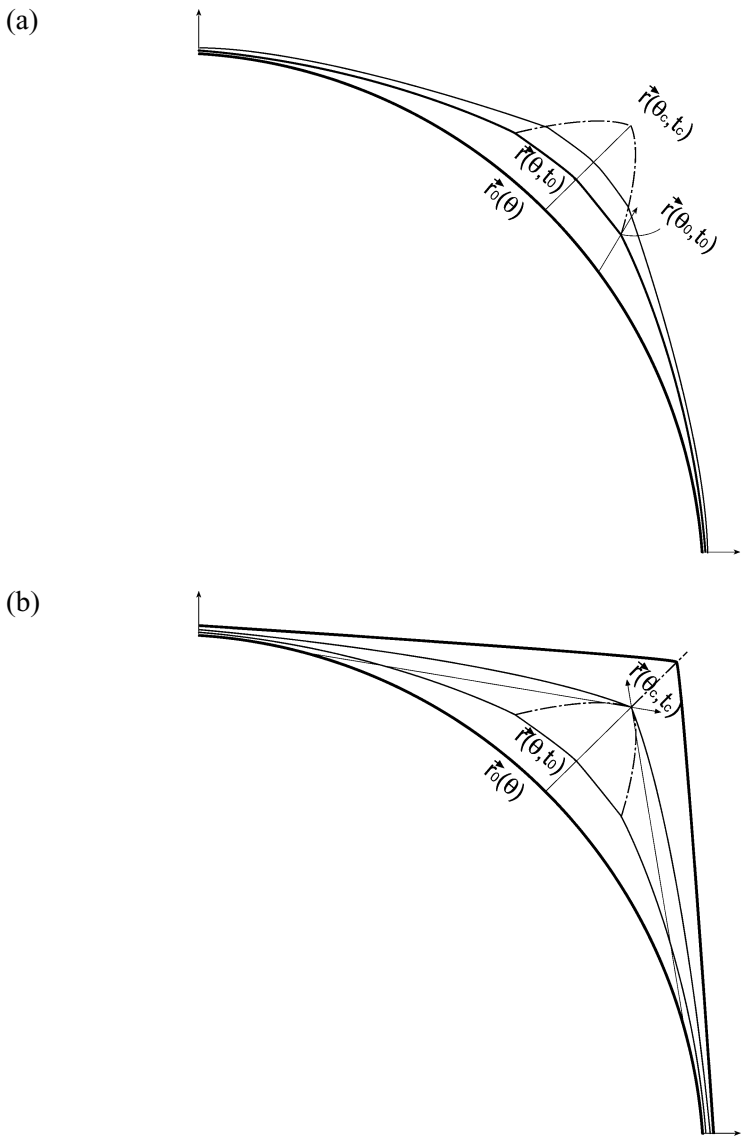

Figure 4. The shape evolution for $V(\theta)$ such that $\tilde{V}(\theta)$ is negative for some range of θ. (a) A shock forms at time $t_0 = -(\kappa_0(\theta_0)\tilde{V}(\theta_0))^{-1}$, and $\tilde{V}$ is a minimum at θ_0. (b) Two shocks on either side of the symmetry orientation $\pi/4$ collide at $t = t_c$ to form a single secondary shock that propagates along the normal at $\theta = \pi/4$. The first orientation whose characteristic hits the secondary shock is θ_c. (c) If conditions for nucleation exist, the primary shocks move toward singular facet orientations $\theta = n\pi/2$. The secondary shocks propagate along the direction of the normals at $\theta = n\pi/2$.

moves in the direction of the normal to the boundary at $\theta = \pi/4$ and continues to absorb vicinal orientations. However, since $V(\theta)$ is symmetric around $\theta = 0$ and differentiable there, $V'(0) = 0$, and the characteristic velocity $\vec{w}(0)$ has the direction of the outward pointing normal at $\theta = 0$. Hence, the characteristic for

(c)

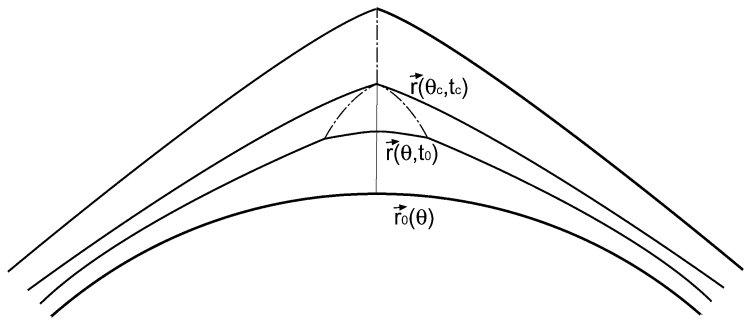

Figure 4. *Continued*.

$\theta = 0$ and, by continuity, some finite range of characteristics corresponding to vicinal orientations, diverge from the secondary shock and never hit it. These orientations remain in the final growth shape. As a result, the latter contains sharp corners at $\theta = \pi/4 + n\pi/2$ and smooth segments at and around $\theta = n\pi/2$.

Geometric models of the crystal growth treat, in particular, the problem of initial shapes which contain orientations below their roughening temperatures [2]. First, consider that the growth drive is sufficiently low and does not exceed the activation barrier for two-dimensional nucleation on the facets. In this case, even if there are no facets on the initial shape, the growth velocity has a global minimum at $\theta = 0$ (e.g., [16]). As we show in Section 4.2, the existence of the global minimum at $\theta = 0$ implies that the surface evolves according to the above scenario with rough orientations ultimately growing out of existence leaving a growth form containing only vicinal orientations. Moreover, under these low growth drive conditions, the growth velocity V_0 at $\theta = 0$ is exponentially small [2]. We expand the normal velocity around $\theta = 0$,

$$V(\theta) \approx V_0 + \alpha\theta^2, \tag{40}$$

where $\alpha = 1/2V_0''$. Then $V'(\theta) \approx 2\alpha\theta$ becomes much larger than $V(\theta)$ at $\theta > \theta_i \sim V_0/\alpha$. Hence, at $\theta > \theta_i$ the characteristic velocity $\vec{w}(\theta) \approx V'(\theta)\vec{T}$, and characteristics run tangential to the boundary and necessarily hit either the primary or secondary shock. Therefore, only orientations $\theta < \theta_i$ remain on the final growth form. For exponentially small V_0, θ_i is very small, and hence the growth shape at large times is very nearly completely faceted, but in fact all surfaces have very small but finite curvature (Figure 4(b)).

If, on the other hand, the growth drive is above the activation barrier for nucleation at all terraces between the steps, including the facet itself, it is plausible that the minimum of $V(\theta)$ at $\theta = 0$ is not global since the nucleation rates can be different at different surface orientations. Then, as we show in Section 4.1, one might encounter a situation wherein at some $t = t_c$, $\theta_2(t_c) = 0$ while $\theta_1(t_c) = \theta_c^{(1)} < \pi/4$. A secondary shock at $t > t_c$ now propagates along the normal at $\theta = 0$, and the resulting growth shape contains sharp corners at

the principal plane orientations ($\theta = n\pi/2$) and well-rounded segments of the boundary at $\theta = \pi/4 + n\pi/2$ (Figure 4(c)).

Now consider an initial shape containing facets at $\theta = n\pi/2$ but no corners. Assume that $V(\theta)$ is differentiable everywhere, having a smooth minimum at $\theta = 0$, while $\tilde{V}(\theta) > 0$ for all θ. Then no shocks are initiated, nonsingular orientations again retain positive curvature during the process of growth, and no corners develop on the surface. The facet moves perpendicular to itself during the entire growth process: since $V(\theta)$ has a smooth minimum at $\theta = 0$, $V'(0) = 0$, and for all points at the facet $\vec{r}(0, t) = -V(0)\vec{N}t$. Moreover, facets do not spread. Because $V(\theta)$ and $V'(\theta)$ are continuous at $\theta = 0$, the characteristic velocity is also continuous everywhere, including the junction between the vicinal orientations and the facet. Therefore, the junction moves in the same direction as the facet itself, and the facet always ends at this junction where it undergoes a continuous (on a larger than microscopic scale) transition into a vicinal surface. The curvature at vicinal orientations decreases with time according to Equation (20), and the corresponding regions look more and more like a facet. However, they never become true facets, and the size of the facet remains constant. Notice, however, that the size of the facet does not stay constant if $V'(\theta)$ is discontinuous at $\theta = 0$ (Section 4.2).

In both of the above scenarios, no instability, as defined by the formation of a concavity, develops if shocks do not form. Even if a shock forms, but neither the initial nor the evolving shape contains facets, the convexity of the surface is preserved. Thus, an initially convex surface remains convex if: (i) no shocks form or (ii) facets are neither present on the initial shape nor develop any time during the evolution. Conversely, there are two conditions that are necessary for a possible development of a surface instability: (i) shock initiation; (ii) a singular (partially faceted) initial shape and/or nondifferentiable $V(\theta)$. While (i) signifies the formation of corners, if condition (ii) is satisfied then either facets are already present on the initial shape or they form and/or spread during the evolution of the surface (Section 4.2).

We also observe that the convexity of the boundary is preserved even if a facet on the growth shape coexists with a propagating shock as long as the normal varies continuously through the junction between the facet and the vicinal orientations, so that there is no macroscopic corner at the edge of the facet (Figure 5(a)). In the presence of a propagating shock two branches of the boundary separated by a corner continue to be convex. Orientations $\theta_2(t) \leq \theta \leq \theta_1(t)$ are absorbed by the corner by time t. One of the branches contains a facet. Since the transition from the facet to the vicinal orientations is continuous, the curved parts of the boundary evolve in the same way as they did for a strictly convex initial shape; no instability of any kind develops. For sufficiently low growth drives, similar to the scenario with a strictly convex initial shape, if at some time $t = t_c$, $\theta_1(t_c) = \pi/4$ while $\theta_2(t_c) = \theta_c^{(2)} > 0$, all rough orientations disappear, while faceted and vicinal surfaces continue to

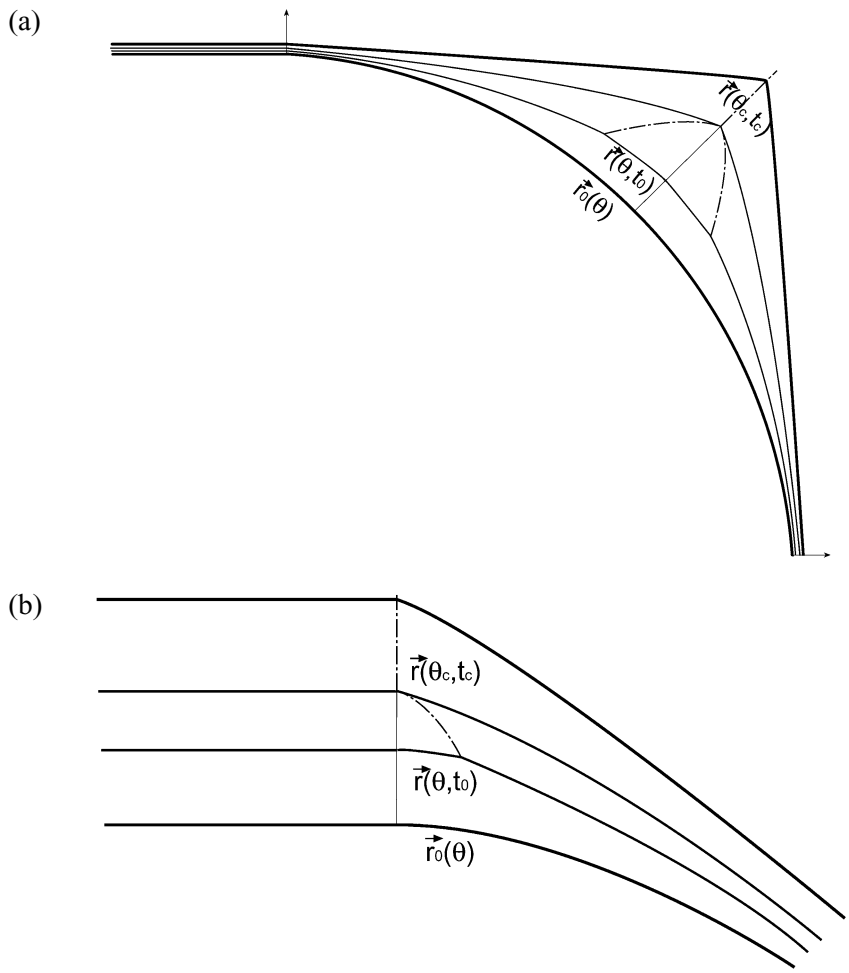

Figure 5. The evolution of an initial shape containing tangentially matching facets, that is, those with a smooth transition to vicinal orientations. Here, $V(\theta)$ is differentiable everywhere, and facets do not spread. (a) The scenario of Figures 4(a) and (b) is repeated. The growth shape at large t is nearly completely faceted. However, only parts of it contain true facets whose width does not change from their sizes on the initial shape. The remainder are vicinal surfaces with very small curvature. (b) When, at time t_c, a shock collides with the facet that grows in the normal direction, a corner forms between the facet and the rough orientations. This is only possible if there are dislocations or if nucleation at the facets exists.

grow. Some of the vicinal orientations are absorbed by a secondary shock; however, the whole facet, as well as a small but finite range of vicinal orientations smoothly adjoining the facet, remain on the final growth shape. The latter represents, therefore, an *almost* completely faceted convex surface.

If, on the other hand, at some time $t = t_c$, $\theta_2(t_c) = 0$ while $\theta_1(t_c) = \theta_c^{(1)} < \pi/4$, a new situation arises (Figure 5(b)): a corner now separates a facet and

the rough orientations. This corner results from the propagation of a shock, which does not stop at the moment when the facet and the shock collide. In fact, the corner continues to sharpen. The trajectory of the shock cannot now be determined by solving Equation (14): a reparameterization of Equation (1) fails since $\vec{r}(0, t)$ has infinitely many values corresponding to various locations on the facet. It is not clear whether the propagation of the shock and its trend to absorb new rough orientations can be reconciled with the requirement that all points on the facet move with the same normal velocity. Otherwise, we may expect the development of an instability.

Thus, we expect that the convexity of the surface may only be broken if at some time during the evolution, the growth shape consists of a facet of finite width at $\theta = 0$ and a rough surface adjoining it, with the two structures separated by a corner. Next, we investigate various functional forms of $V(\theta)$ that could lead to the formation of a corner separating a facet and a rough segment of the boundary. We treat the two cases separately, one that is described by $V(\theta)$ which has a continuous derivative everywhere, the other characterized by $V(\theta)$ which has a cusp at $\theta = 0$. These two cases cover all possible functional forms of $V(\theta)$. Having proven that a corner at the edge of the facet never leads to the formation of concavity in both of the above situations, we have then exhausted all possible scenarios of surface evolution, completing the proof that the geometric evolution equation (1) preserves the convexity of the surface.

4.1. Differentiable $V(\theta)$

We first assume that the initial shape contains facets and that $V(\theta)$ is differentiable everywhere. As discussed above, differentiability implies $V'(0) = 0$. When the shock collides with the facet, the last vicinal orientation disappears, and some characteristic corresponding to θ_c somewhat smaller than $\pi/4$ crosses the outermost facet characteristic associated with $\theta = 0$. In this case, in Equation (39) $\theta_1 = 0$, $\Delta\theta = \theta_c$, and $V'(\theta_1) = 0$. The condition for the collision of the shock and the facet then reads

$$V(0) = V(\theta_c) - V'(\theta_c) \tan \frac{\theta_c}{2}. \tag{41}$$

In Equation (41), $\theta_c \approx \pi/4$, and $\tan \theta_c/2 \approx 0.414$, i.e., not small. Therefore, Equation (41) implies that the shock collides with the facet only if the normal growth velocity at the rough orientations close to $\pi/4$ has the same order of magnitude as that at the facet. This cannot happen for dislocation-free crystals at growth drives below the activation barrier for two-dimensional nucleation at the facets: facets grow due to nucleation processes, and hence $V(0)$ is exponentially small. The growth velocity at rough orientations, on the other hand, depends linearly on the growth drive, and is therefore much larger than $V(0)$ at sufficiently low growth drives.

However, if there are dislocations leading to the finite density of steps on the facet and the normal velocity of the facet is proportional to the growth drive [13, 16] or if growth drives are large enough to exceed the activation barrier, and hence lead to a facet growth rate that is comparable with that at the rough orientations, Equation (41) implies that facets may collide with the shock. Nevertheless, as we show next, such a collision does not lead to the formation of concavities.

All locations on the facet move in the same direction perpendicular to the facet with the same characteristic velocity $\vec{w} = -V_0\vec{N}$. The trajectories of the facet points are

$$\vec{r}_{x_0}(0, t) = \vec{r}_0(\theta) + \vec{w}t, \tag{42}$$

where each trajectory is labeled by the x-coordinate of its starting point. At the moment t_c when the shock collides with the facet, the outermost facet characteristic intersects one associated with some rough orientation θ_c. The shock continues to propagate if the pairs of intersecting characteristics continue to exist at $t > t_c$. The members of the pairs are trajectories of the orientations with $\theta > \theta_c$, on the one hand, and the facet characteristics on the other. Figure 6 shows that if such pairs can be found, the coordinate of the starting point of the intersecting facet characteristics, x_0, decreases with time.

We now treat x_0 and θ as functions of time in the same way we did when deriving Equation (14). With the axes chosen as shown in Figure 6, we can write the condition for the intersection of two characteristics $\vec{r}_{x_0(t)}(0, t) = \vec{r}(\theta(t), t)$ as

$$x_0(t)\hat{x} - V_0 t\hat{y} = \vec{r}_0(\theta(t)) + (-V(\theta(t))\vec{N} + V'(\theta(t))\vec{T})t. \tag{43}$$

Therefore,

$$x_0(t) = r_0 \sin\theta + (V \sin\theta + V' \cos\theta)t, \tag{44}$$

and

$$-V_0 t = r_0(1 - \cos\theta) + (-V \cos\theta + V' \sin\theta)t. \tag{45}$$

Differentiating Equation (43) with respect to time we obtain

$$\frac{dx_0}{dt} = \frac{1}{\kappa_0}(1 + \tilde{V}\kappa_0 t)\cos\theta\frac{d\theta}{dt} + (V \sin\theta + V' \cos\theta), \tag{46}$$

and

$$-V_0 = \frac{1}{\kappa_0}(1 + \tilde{V}\kappa_0 t)\sin\theta\frac{d\theta}{dt} + (-V \cos\theta + V' \sin\theta). \tag{47}$$

From Equation (45) we get

$$\frac{d\theta}{dt} = \frac{-V_0 + (V \cos\theta - V' \sin\theta)}{(1 + \tilde{V}\kappa_0 t)\sin\theta}\kappa_0, \tag{48}$$

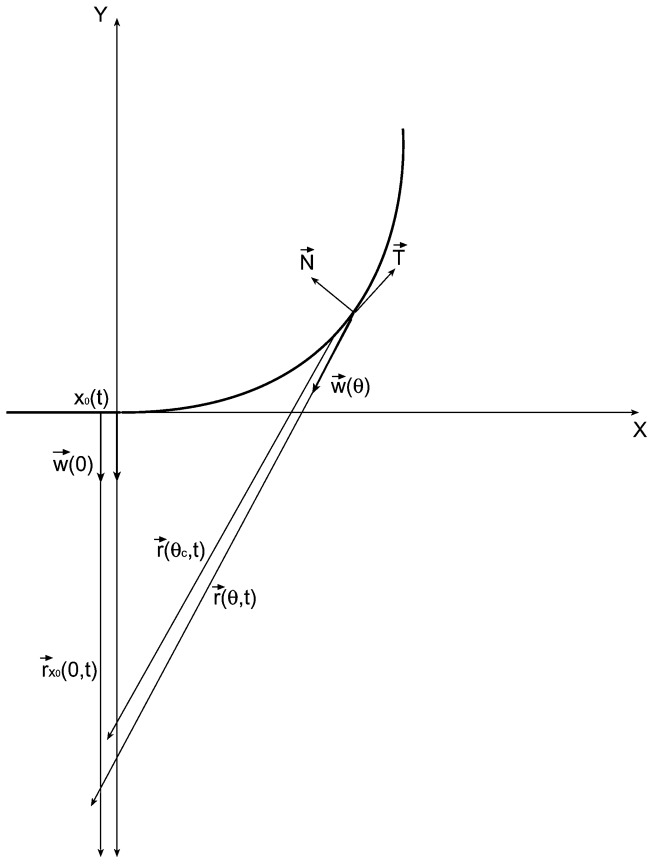

Figure 6. A shock collides with the facet at time t_c when a rough orientation characteristic $\vec{r}(\theta_c, t)$ intersects the outermost facet characteristic. If the shock continues to propagate for $t > t_c$, the coordinate x_0 of the point where the rough orientation characteristics intersect facet characteristics decreases with time.

and hence

$$\frac{dx_0}{dt} = (-V_0 + V\cos\theta - V'\sin\theta)\cot\theta + V\sin\theta + V'\cos\theta$$
$$= -V_0\cot\theta + \frac{V}{\sin\theta}. \tag{49}$$

We first show that the moment the shock collides with the facet, x_0 starts to move in the negative x-direction facilitating the continued propagation of the shock. The rough orientation characteristic θ_c that intersects the trajectory of the endpoint of the facet is determined by Equation (41) from which it follows that

$$\tan\frac{\theta_c}{2} = -\frac{V_0 - V}{V'}. \tag{50}$$

Writing Equation (49) as

$$\frac{dx_0}{dt} = \frac{1}{\sin\theta}(-V_0\cos\theta + V), \tag{51}$$

and noting that $\sin\theta_c > 0$, we observe that the sign of dx_0/dt at the moment of collision is determined by the sign of $-V_0\cos\theta_c + V(\theta_c)$. Expressing $\cos\theta_c$ via $\tan\theta_c/2$, we obtain

$$\begin{aligned} -V_0\cos\theta_c + V &= -V_0\frac{V'^2 - (V_0 - V)^2}{V'^2 + (V_0 - V)^2} + V \\ &= \frac{(V_0 - V)\left(V_0^2 - V^2 - V'^2\right)}{V'^2 + (V_0 - V)^2}, \end{aligned} \tag{52}$$

where all functions are evaluated at θ_c. Because the characteristic for θ_c intersects the characteristic associated with the facet orientation, its velocity has a negative tangential component (Figure 6), and hence, $V'(\theta_c) < 0$. Since $\tan\theta_c/2 > 0$ we conclude from Equation (50) that $V_0 > V$. Then the expression in Equation (52) is negative, $dx_0/dt < 0$, and immediately after colliding with the facet the shock continues to propagate.

To conclude the proof of the preservation of convexity we show that the direction of motion of x_0 never changes. From Equation (45) we find that the intersection time for the characteristic corresponding to the orientation θ is

$$t = \frac{1}{\kappa_0(\theta)}\frac{1 - \cos\theta}{(-V_0 + V\cos\theta - V'\sin\theta)}. \tag{53}$$

The shock propagates only if $0 < t < \infty$, which implies that we should only consider orientations $\theta < \theta_f$, where θ_f is the root of the denominator in Equation (53). For these orientations,

$$-V_0 + V\cos\theta - V'\sin\theta > 0. \tag{54}$$

The above result is consistent with Equation (48) which then implies that θ grows with time. Computing the second derivative of x_0 with respect to time, we obtain

$$\begin{aligned} \frac{d^2x_0}{dt^2} &= \frac{d}{dt}\frac{dx_0}{dt} \\ &= \left(\frac{V_0}{\sin^2\theta} + \frac{V'}{\sin\theta} - \frac{V\cos\theta}{\sin^2\theta}\right)\frac{d\theta}{dt} \\ &= (V_0 + V'\sin\theta - V\cos\theta)\frac{1}{\sin^2\theta}\frac{d\theta}{dt}. \end{aligned} \tag{55}$$

According to Equation (54), the expression in the brackets is negative, while the other two factors are positive. Therefore, d^2x_0/dt^2 is negative. Since dx_0/dt is negative at $t = t_c$, we conclude that it is negative for all $t > t_c$ as well,

and x_0 moves in the negative x-direction for all time. Hence, an intersection pair can be found for all $t > t_c$, and no instability arises.

The denominator in Equation (53) approaches zero as $\theta \to \theta_f$, which implies that only orientations $\theta < \theta_f$ can be eliminated by the shock, and the rest remain in the final growth shape. The final growth shape consists of the corners at principal facet orientations connected by smooth curves with very small curvature. Incidentally, such a growth shape has recently been observed in the melting of a small ice crystal [28].

4.2. Surface evolution in the case when $V(0)$ has a cusp

Any growth process wherein interfacial kinetics control the advance of the surface can be described by a geometric model. Within the models we have seen so far the facets do not spread. However, many experiments performed at growth drives too weak to induce kinetic roughening and at temperatures below the roughening transition of the facet orientations (conforming with the conditions of geometric growth), have resulted in a completely faceted growth shape. Most recently, Maruyama et al. [20] observed faceting of CCl_4-crystals during interfacially controlled growth. It appears that the spreading of the facet is captured by the geometric evolution model, Equation (1), wherein the growth velocity $V(\theta)$ contains a true cusp at facet orientations.

The equilibrium shape of a crystal at temperatures below the roughening transition contains facets. The presence of facets on the equilibrium shape indicates that the surface free-energy function $\gamma(\theta)$ has a discontinuous derivative at $\theta = n\pi/2$ [16]. By analogy, it is reasonable to assume that under the same conditions $V(\theta)$ has a cusp at facet orientations. It is well known, for example, that for layer-by-layer growth of a crystal, the growth velocity $V(\theta)$ does have a cusp at $\theta = n\pi/2$ [16]. In general, if the growth of the surface is governed by the motion of steps along the surface, $V(\theta)$ necessarily has a cusp at facet orientations: the velocity v of the steps adjacent to the facet is finite, so that the normal velocity $V(\theta) = v \sin\theta$ decreases linearly at small θ, its derivative being finite. Alternatively, since the facet practically does not move perpendicular to itself, and the steps at the end of the facet move parallel to it with the finite speed, the facet spreads.

Next we examine the effect the existence of a cusp in $V(\theta)$ has on surface evolution keeping in mind that the temperature is sufficiently low and the growth drive is sufficiently weak to make the growth velocity of the facet orientations exponentially small. Any cusp in V ($V'(\theta^-) \neq V'(\theta^+)$) leads to a discontinuity in $\vec{w}$, the velocity along the characteristic at $\theta = 0$, since $\vec{w} = -V(\theta)\vec{N} + V'(\theta)\vec{T}$. All points on the original facet move perpendicular to the surface with a very small velocity. Two characteristics originate from the point where the facet ends: $\vec{r}(0, t)$ corresponding to the outermost facet location that moves normal to the surface with velocity $\vec{w}(0) = -V(0)\vec{N}$, and $\vec{r}(0^+, t)$ associated with the

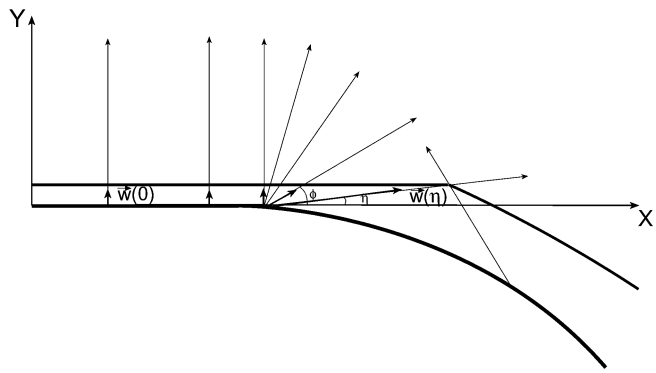

Figure 7. A fan emanates from the edge of the facet if $V(\theta)$ has a cusp at $\theta = 0$. All fan characteristics have the same, exponentially small, y-component of the velocity equal to the normal growth velocity of the facet $V(0)$. We denote ϕ as the angle formed by a fan characteristic with the horizontal axis, and η is a similar angle formed by the outermost fan characteristic. We note that η is exponentially small.

first vicinal orientation moving with velocity $\vec{w}(0^+) = -V(0)\vec{N} + V'(0^+)\vec{T}$ at an angle η to the normal, such that $\tan\eta = V'(0^+)/V(0)$. To fill the void between two characteristics, a fan has to be introduced [1] (Figure 7). Physically, new segments of the boundary continuously emerge at the edge of the facet. It is easy to see that for a stable convex curve these new segments can only extend the facet: the normal has the same orientation ($\theta = 0$) along the characteristics $\vec{r}(0, t)$ and $\vec{r}(0^+, t)$, and therefore has to be the same everywhere between them. As a result, the facet spreads. The endpoint of the facet moves along the trajectory of the first vicinal orientation. The rate of spreading is determined by the tangential component of the velocity $\vec{w}(0^+)$. Thus, the facet spreads with velocity $V'(0^+)$.

Spreading of the facet necessarily leads to a completely faceted growth shape wherein the edges of the facets at two adjacent principal faces, e.g., at $\theta = 0$ and $\theta = \pi/2$, move in perpendicular directions toward each other with equal speed and hence, collide in finite time. On the other hand, a completely faceted shape, where all rough orientations are absent, can only be the result of the propagation of a shock that absorbs all rough orientations. The shock is initiated at time t_0 at the point of the global minimum of $\tilde{V}$. As the shock propagates new characteristics are terminated, and the corner approaches the facet. After the last vicinal orientation is eliminated by the corner the facet collides with the shock. At this moment the facet becomes immediately adjacent to a rough orientation and is separated from it by a corner.

Now we discuss a simple model of $V(\theta, \delta\mu)$ that captures all the features described above as well as qualitatively reproduces evolution observed experimentally [20]. Here $\delta\mu$ is the chemical potential difference between the bulk phases in contact which is assumed to be spatially and temporally uniform. In particular,

we define a local normal velocity $V(\theta, \delta\mu)$ that: (i) is periodic in $\pi/2$ and preserves the four-fold symmetry of the surface; (ii) has a nonzero derivative at $\theta = 0$; (iii) leads to a negative $\tilde{V}$ at vicinal orientations and, possibly, positive $\tilde{V}$ at the roughest orientations; (iv) describes activated growth at the facets. The simplest form of $V(\theta, \delta\mu)$ possessing the above properties is [2]

$$V(\theta, \delta\mu) = V_f(\delta\mu)\xi(\theta) + V_r(\theta, \delta\mu). \tag{56}$$

Here $V_f(\delta\mu)$ is the normal growth rate at facet orientations

$$V_f(\delta\mu) = c_f g(\delta\mu) \exp\left(-\frac{\pi\sigma^2}{kT\delta\mu}\right), \tag{57}$$

whereas for nonsingular orientations we express the linear response to the growth drive as

$$V_r(\theta, \delta\mu) = c_r\delta\mu(a\,|\sin 2\theta| - b\sin^2 2\theta). \tag{58}$$

In the above expressions σ is the free energy of a critical nucleus on the facet (e.g., [29]), T is the temperature, and $\xi(\theta)$ is a smooth periodic function with period $\pi/2$, and the properties $\xi(0) = 1$ and $\xi(\pi/4) = 0$. In contrast to the form of $V(\theta, \delta\mu)$ suggested earlier [2], Equation (56) incorporates a cusp at singular orientations.

At low temperatures $V(\theta) \approx V_r$,

$$\tilde{V} = -3a\sin 2\theta - b(\sin^2 2\theta + 8\cos 4\theta), \tag{59}$$

and

$$V(0) = 0, \tag{60}$$

$$V'(0) = 2a, \tag{61}$$

$$\tilde{V}(0) = -8b,\ \tilde{V}(\pi/4) = 7b - 3a. \tag{62}$$

Since $\tilde{V}(0) < 0$, the curvature at vicinal orientations grows with time. If, however, $a < 7/3b$, the roughest orientations evolve with *decreasing* curvature. We also find that $V(\theta)$ has extrema at $\theta = \pi/4$ and $\theta = 1/2\sin^{-1} a/2b$. If $a < 2b$, $V(\theta)$ has a minimum at $\theta = \pi/4$ which can possibly be ascribed to a thermal diffusion flux toward singular orientations [2, 30, 31]. For $a > 2b$, on the other hand, $V(\theta)$ grows monotonically with θ and is a maximum at $\pi/4$. Thus, models with $2b < a < 7/3b$ describe a physical situation wherein the formation and expansion of the facets is accompanied by decreasing curvature at rough orientations, even though surface diffusion may not introduce a critical change to the normal growth velocity keeping it maximum where the step density is the highest.

From Equation (59) we also find that $\tilde{V}$ has a minimum at $\theta_0 = 1/2\sin^{-1} 3a/31b$. For $2b < a < 7/3b$, $\theta_0 \sim 0.1$, meaning that the shock is initiated in the immediate vicinity of the facet. It is easy to see that if t_0 is the time

of corner formation, the facet collides with a shock at $t \sim 1.1t_0$, which is almost immediately after the initiation of the shock. Interestingly enough, this is exactly the situation observed in [20].

Finally, let us note that Equation (56) is consistent with the general conclusions of the layer-by-layer surface growth described by the motion of the steps [16, 32]. According to the theory, the step velocity v_s is a monotonically increasing function of the terrace width; in other words, v_s is a monotonically decreasing function of θ. Recalling that $v_s(\theta) = V(\theta)/\sin\theta$, and analyzing $v_s(\theta)$ with $V(\theta)$ from Equation (58), we find that for $2b < a < 7/3b$, $v_s(\theta)$ is indeed a decreasing function.

Thus far we have shown that the case when the facet forms a corner with rough orientations for a differentiable $V(\theta)$ does not result in any kind of instability. Next, we discuss the solution for a similar situation but for a cusped $V(\theta)$. We seek a stable solution to the evolution equation assuming that at time $t = t_1$ the corner collides with the facet. As we have shown in Section 3, the trajectory of the shock at $t < t_1$ is determined by intersecting pairs of characteristics, one on each side of the shock trajectory. For $t > t_1$ the facet ends at a corner, and the trajectory of the shock coincides with that of the facet endpoint. As mentioned above, the solution of the evolution equation for any t contains a fan of characteristics emanating from the endpoint of the facet. The fan consists of a continuous set of straight lines forming angle ϕ with the x-axis such that $\phi_{\min} < \phi < \phi_{\max}$, $\phi_{\min} = \tan^{-1}\eta$, and $\phi_{\max} = \pi/2$ (Figure 7). At $t > t_1$ the only characteristics left on the facet side of the corner are those of the fan and a continuous set of facet characteristics. Since, as we have shown above, facet characteristics do not intersect the rough ones below the facet-roughening transition, a shock trajectory at $t \geq t_1$ is determined by a pair of characteristics intersecting at time t, one corresponding to a rough orientation, the other belonging to the fan.

The problem of finding such a pair is similar to the one we solved above. However, it is significantly simplified by the fact that most of the fan characteristics are practically tangential to the facet. To see this notice that since the effect of the fan is to spread the facet, all of the fan's characteristics have the same normal velocity component w_y, equal to $V(0)$: all of them originate at the same point, and for every t the y-coordinate along each of them is equal to that of the facet. Thus, only the component of the velocity tangential to the facet w_x is different for various characteristics within the fan, varying between zero in the interior of the facet and $V'(0^+)$ for the fan's outermost characteristic. The angle ϕ that each characteristic forms with the x-axis is $\phi = \tan^{-1}(w_y/w_x)$. At low growth drives $V(0)$ is exponentially small, and the angle η between the fan's outermost trajectory and the x-axis is equal to $\pi/2$ up to an exponentially small correction. Moreover, all those characteristics for which $w_x \gg w_y$ are also indistinguishable from actually being tangential to the facet. Therefore, as long as $w_x \gg V(0)$, i.e., the characteristic velocity is

not exponentially small, the fan characteristic can be considered to be running along the facet. In other words, all fan characteristics that may intersect with a rough orientation characteristic are tangential to the facet.

As a consequence, for the purpose of finding the trajectory of the shock we treat the facet as pinned and immobile in the y-direction, while spreading along the x-axis due to the fan. The latter initially consists of characteristics running along the facet with velocities ranging from 0 to $V'(0^+)$. The shock continues to propagate at $t > t_1$ if at any $t > t_1$ the fastest of the surviving fan characteristics finds an intersecting pair among the rough orientation characteristics and is thereby eliminated by the shock. If the shock continues to propagate, its trajectory is collinear with the facet for $t > t_1$. As a result of shock propagation, the speed of the outermost surviving characteristic within the fan decreases with time. Since the facet spreads with the speed of the outermost (the fastest) characteristic, spreading slows down as well.

We choose the coordinate system so that the x-axis coincides with the facet (Figure 8). According to the above discussion we assume that the facet does not move in the y-direction. We assume further that there is a shock after $t = t_1$. Since it propagates along the straight line containing the facet, we have $y = 0$ along the shock trajectory. The characteristic associated with the rough

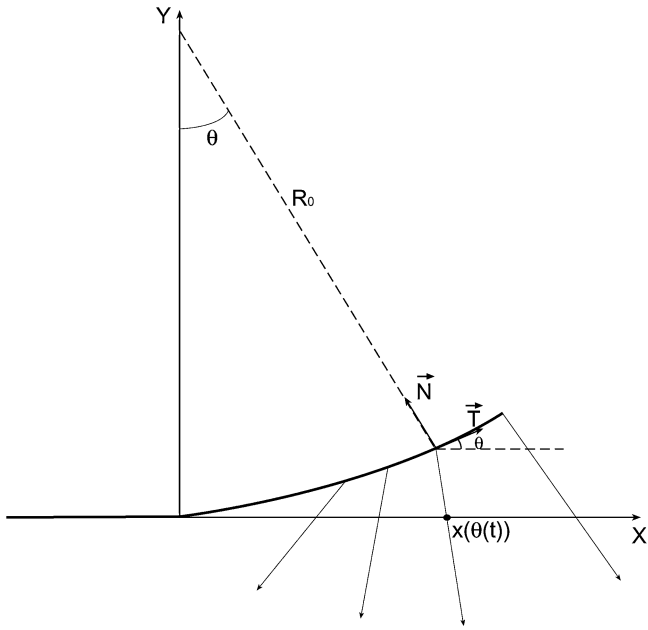

Figure 8. Motion of the edge of the facet after it collides with the shock. To determine the position of the corner at the edge of the facet at time t, we need to find the orientation θ whose characteristic intersects the line $y = 0$ at time t, and calculate the x-coordinate along this characteristic at time t.

orientation θ that has not been eliminated by the shock until $t = t_1$, intersects the line $y = 0$ at the point with coordinate $x(\theta)$. Similar to what we showed in Section 3, we define a function $\theta(t)$ that determines the orientation absorbed by the shock at time t. We can therefore consider a function $x = g(t)$ that defines the coordinate of the intersection point as a function of time. It also defines the trajectory of the shock. However, since the fan characteristics are absorbed by the shock and the speed of the outermost characteristic decreases with time, the same should happen with the velocity of the shock. In other words, the shock trajectory coincides with that of the endpoint of the facet whose instantaneous velocity is determined by the speed of the outermost fan characteristic. Since the latter decreases with time, so does the shock velocity dg/dt. Therefore, the shock continues to propagate if the condition

$$\frac{d^2g}{dt^2} < 0 \tag{63}$$

is satisfied.

Next, we prove that condition Equation (63) is satisfied at all times and for any $V(\theta)$. For simplicity we again treat a circular initial shape. Using $\vec{r}(\theta, t) = \vec{r}_0(\theta) + \vec{w}(\theta)t$, $\vec{w} = -V(\theta)\vec{N} + V'(\theta)\vec{T}$, and $\vec{r}_0(\theta) = (x_0(\theta), y_0(\theta))$, we first find the time t_s when the characteristic corresponding to a rough orientation θ intersects the line $y = 0$. It is determined by solving the equation

$$y_0(\theta) + w_y(\theta)t_s = 0. \tag{64}$$

Noting that $\vec{N} = (-\sin\theta, \cos\theta)$, $\vec{T} = (\cos\theta, \sin\theta)$, and $y_0(\theta) = R_0(1 - \cos\theta)$ (see Figure 8), we write

$$R_0(1 - \cos\theta) + (-V(\theta)\cos\theta + V'(\theta)\sin\theta)t_s = 0. \tag{65}$$

It follows that

$$t_s(\theta) = \frac{R_0(1 - \cos\theta)}{V(\theta)\cos\theta - V'(\theta)\sin\theta}, \tag{66}$$

which is meaningful only if $t_s > 0$. (We return to the implications of Equation (66) later.)

Since $x_0(\theta) = R_0 \sin\theta$, the x-coordinate of the intersection point is determined by

$$\begin{aligned} x_s(\theta) &= R_0\sin\theta + (V(\theta)\sin\theta + V'(\theta)\cos\theta)t_s(\theta) \\ &= R_0\sin\theta + \frac{V(\theta)\sin\theta + V'(\theta)\cos\theta}{V(\theta)\cos\theta - V'(\theta)\sin\theta}R_0(1 - \cos\theta) \\ &= R_0\frac{V(\theta)\sin\theta - V'(\theta)(1 - \cos\theta)}{V(\theta)\cos\theta - V'(\theta)\sin\theta}. \end{aligned} \tag{67}$$

By definition of the function $g(t) = x_s(\theta(t))$ for any t. Then we find

$$\frac{dg}{dt} = \frac{dx_s(t)}{d\theta}\frac{d\theta}{dt}. \tag{68}$$

At this stage we determine $d\theta/dt$ by differentiating Equation (65) with respect to the independent variable t as follows:

$$R_0 \sin\theta \frac{d\theta}{dt} + (-V(\theta)\cos\theta + V'(\theta)\sin\theta) + \tilde{V}(\theta)t\sin\theta\,\frac{d\theta}{dt} = 0, \tag{69}$$

or, expressing the time of intersection in terms of the corresponding angle,

$$\begin{aligned}\frac{d\theta}{dt} &= \frac{V(\theta)\cos\theta - V'(\theta)\sin\theta}{(R_0 + \tilde{V}(\theta)t)\sin\theta} \\ &= \frac{1}{R_0\sin\theta}\frac{(V(\theta)\cos\theta - V'(\theta)\sin\theta)^2}{V(\theta)\cos\theta - V'(\theta)\sin\theta + \tilde{V}(\theta)(1-\cos\theta)}.\end{aligned} \tag{70}$$

Next, we find $dx/d\theta$ from Equation (67), and omitting the intermediate algebraic steps, we obtain

$$\begin{aligned}\frac{dx(t_s)}{d\theta} &= \frac{R_0 V(\theta)}{(V(\theta)\cos\theta - V'(\theta)\sin\theta)^2} \\ &\quad \times [V(\theta)\cos\theta - V'(\theta)\sin\theta + \tilde{V}(\theta)(1-\cos\theta)].\end{aligned} \tag{71}$$

Combining Equation (70) with Equation (71) we find a very simple expression for dg/dt

$$\frac{dg}{dt} = \frac{V(\theta)}{\sin\theta}, \tag{72}$$

where $\theta = \theta(t)$ is a known function. Finally, we compute the second derivative d^2g/dt^2 to find

$$\begin{aligned}\frac{d^2g}{dt^2} &= \frac{d}{d\theta}\left(\frac{V(\theta)}{\sin\theta}\right)\frac{d\theta}{dt} \\ &= -\frac{V(\theta)\cos\theta - V'(\theta)\sin\theta}{\sin^2(\theta)}\,\frac{d\theta}{dt}.\end{aligned} \tag{73}$$

In Equation (73) $d\theta/dt > 0$: by definition $\theta(t)$ is an increasing function of time. We also conclude from (66) that in order for $t_s > 0$, the condition

$$V(\theta)\cos\theta - V'(\theta)\sin\theta > 0 \tag{74}$$

has to be satisfied. Since $d\theta/dt > 0$, the same condition is necessary and sufficient for $d^2g/dt^2 < 0$. It is easy to prove that (74) is always true.

Assume that there is only one corner forming in the process of evolution, that at $t = t_1$ the shock collides with the facet, and that $\theta(t_1) = \theta_1$. Then $t_s(\theta_1) = t_1 > 0$, and therefore $V(\theta_1)\cos\theta_1 - V'(\theta_1)\sin\theta_1 > 0$. Now consider

the possibility that for the $\theta_2 > \theta_1$ condition Equation (74) ceases to be satisfied, and $V(\theta_2)\cos\theta_2 - V'(\theta_2)\sin\theta_2 = 0$. Since $f(\theta) = V(\theta)\cos\theta - V'(\theta)\sin\theta$ is positive for θ_1 and becomes zero at θ_2, it has to decrease as θ approaches θ_2. Then $f'(\theta) = -\tilde{V}(\theta)\sin\theta$ is negative within some vicinity of θ_2: $\theta_2 - \Delta < \theta < \theta_2$. Therefore, $\tilde{V}(\theta) > 0$ within this vicinity. In the case of only one corner developing on the crystal surface, $\tilde{V}(\theta)$ may only have one (negative) minimum at θ_0, where the shock is initiated, $\theta_0 < \theta_1 < \theta_2$. For $\theta > \theta_0$, $\tilde{V}(\theta)$ is an increasing function. Then, from $\tilde{V}(\theta_2) > 0$ we conclude that $\tilde{V}(\theta) > 0$ for all angles $\theta_2 \leq \theta \leq \pi/4$. It follows that $f(\theta)$ monotonically decreases from θ_2 to $\pi/4$. Being zero at θ_2, it is therefore negative everywhere within $\theta_2 < \theta \leq \pi/4$. We are then forced to conclude from (66) that no characteristic in the range $\theta_2 < \theta \leq \pi/4$ intersects the line $y = 0$ at positive times. However, this is not true at least for the characteristic corresponding to $\pi/4$: it is normal to the surface and necessarily intersects the line $y = 0$ at a positive time (see Figure 8). This contradiction indicates that if only one shock develops in the process of shape evolution, d^2g/dt^2 is always negative, and for any $t > t_1$ there exists an intersecting pair of characteristics one member of which corresponds to the rough orientation and the other of which belongs to the fan. Therefore the shock continues to propagate after $t = t_1$ until the shape becomes fully faceted.

Allowing more complicated functional dependences of $V(\theta)$ may result in the appearance of more than one corner but does not alter the general result that a proper $g(t)$ can always be constructed and the shock continues to propagate. For example, if two corners coexist for some time during the evolution process, one of the shocks still propagates along $y = 0$ after colliding with the facet. The other shock necessarily moves toward the facet, and in finite time is absorbed by the "shocking" facet that continues to spread parallel to itself.

Finally, any form of the normal growth velocity function $V(\theta)$ can be represented as a linear combination of two functions: $V_1(\theta)$ that is differentiable everywhere and has a minimum at $\theta = 0$, and $V_2(\theta)$ that is zero $\theta = 0$ and has a cusp at singular orientations. In fact, the only form of $V(\theta)$ that has not been discussed explicitly so far is the one that has a cusp at $\theta = 0$ and is nonzero there. However, in the frame of reference moving with velocity $V(0)$ in the direction perpendicular to the facet, the growth function $V(\theta)$ in Equation (1) has exactly the form of $V_1(\theta)$ for which the convexity is preserved. Thus we conclude that Equation (1) preserves convexity of the interface for any form of the growth function $V(\theta)$ and any initial shape.

5. Conclusions

We have investigated a geometric approach to the kinetics associated with highly anisotropic crystal growth. We have shown that only one type of surface singularity can be realized in geometric evolution, namely, a jump of

the normal that leaves the curvature finite on both sides of the jump. We proved that the shock, leading to such a singularity, eliminates the possibility of a continuous limiting process of curvature divergence wherein the curvature is infinite on both sides of the singular point. By exhausting all possible scenarios we were also able to show that if the initial seed crystal is convex, it remains convex during the entire growth process. This conclusion is valid for a wide range of growth shapes including partially faceted crystals and those containing corners. We also explained how different models for the growth velocity V describe a variety of growth shapes observed in nature. In particular, we presented a form of V having a cusp at faceted orientations that explains the formation of a "shocking facet"—an expanding facet separated from the rough orientations by a corner. Such a development has recently been observed [28].

Finally, we would like to note that some interesting phenomena observed during the later stages of crystal growth, such as dynamic faceting sometimes followed by the formation of concavities, cannot be described within the geometric model. These instabilities have a dynamic origin, while the geometric model is kinematic in nature and is well suited for explaining the earlier stages of growth. Analysis of these dynamical phenomena is the subject of another study [33].

References

1. J. Taylor, J. W. Cahn, and C. A. Handwerker, Geometric models of crystal growth, *Acta Metall*. 40:1443 (1992) reviews geometric models.
2. J. S. Wettlaufer, M. Jackson, and M. Elbaum, A geometric model of anisotropic crystal growth, *J. Phys. A* 27:5957 (1994).
3. A. L. Bertozzi, M. P. Brenner, T. F. Dupont, and L. P. Kadanoff, Singularities and similarities in interface flows, in *Trends and Perspectives in Applied Mathematics*, Vol. 100 *Applied Mathematical Sciences* (L. Sirovich, Ed.), pp. 155–208, Springer-Verlag, New York, 1994.
4. R. E. Goldstein, A. I. Pesci, and M. J. Shelley, Attracting manifold for a viscous topology transition, *Phys. Rev. Lett*. 75:3665 (1995).
5. S. M. Allen and J. W. Cahn, A microscopic theory for antiphase boundary motion and its application to antiphase domain coarsening, *Acta Metall*. 27:1085 (1979).
6. S. A. Langer, R. E. Goldstein, and D. P. Jackson, Dynamics of labyrinthine pattern-formation in magnetic fluids, *Phys. Rev. A* 46:4894 (1992).
7. P. W. Voorhees, The theory of Ostwald ripening, *J. Stat. Phys*. 38:231 (1985).
8. D. M. Petrich and R. E. Goldstein, Nonlocal contour dynamics model for chemical front motion, *Phys. Rev. Lett*. 72:1120 (1994).
9. K. Nakayama, H. Segur, and M. Wadati, Integrability and the motion of curves, *Phys. Rev. Lett*. 69:2603 (1992); R. E. Goldstein and D. M. Petrich, The Korteweg-deVries hierarchy as dynamics of closed curves in the plane, *Phys. Rev. Lett*. 67:3203 (1991).
10. R. Brower et al., Geometrical approach to moving-interface dynamics, *Phys. Rev. Lett*. 51:1111 (1983); R. Brower et al., Geometrical models of interface evolution, *Phys.*

Rev. A 29:1335 (1984); J. S. LANGER, Lectures in the theory of pattern formation, in *Chance and Matter* (J. Souletie, J. Vannimenus, and R. Stora, Eds.), North Holland, New York (1987) (also reviews some geometric models); D. A. KESSLER, J. KOPLIK, and H. LEVINE, Pattern selection in fingered growth phenomena, *Adv. Phys*. 37:255 (1988); E. BEN-JACOB and P. GARIK, The formation of patterns in nonequilibrium growth, *Nature* 343:523 (1990); E. YOKOYAMA and R. SEKERKA, A numerical study of the combined effect of anisotropic surface-tension and interface kinetics on pattern formation during the growth of 2-dimensional crystals, *J. Cryst. Growth* 125:389 (1992).

11. S. ANGENENT and M. E. GURTIN, Multiphase thermomechanics with interfacial structure. 2. Evolution of an isothermal interface, *Arch. Ration. Mech. Anal*. 104:323 (1989); M. A. GRAYSON, The heat-equation shrinks embedded plane curves to round points, *J. Diff. Geom*. 26:285 (1987); M. GAGE and R. S. HAMILTON, The heat-equation shrinking convex plane curves, *J. Diff. Geom*. 23:69 (1986).
12. G. WULFF, Zur frage der Geschwindigkeit des Wachstums und der Auflosung der Krystalflachen, *Z. Krystallogr. Mineral*. 34:499 (1901).
13. F. C. FRANK, On the kinematic theory of crystal growth and dissolution processes, in *Growth and Perfection of Crystals* (R. H. Doremus, B. W. Roberts, and D. Turnbull, Eds.), Wiley, New York, 1958.
14. F. C. FRANK, On the kinematic theory of crystal growth and dissolution processes, II, *Z. Phys. Chem. N.F.* 77:84 (1972).
15. J. VILLAIN, Nonequilibrium systems—The shape of crystals to come, *Nature* 350:273 (1991).
16. A. A. CHERNOV, *Modern Crystallography III, Crystal Growth*, Springer, Berlin (1984), 122.
17. J. C. HEYRAUD and J. J. MÉTOIS, Growth shapes of metallic crystals and roughening transition, *J. Cryst. Growth* 82:269 (1987).
18. J. TERSOFF, A. W. DENIER VAN DER GON, and R. M. TROMP, Shape oscillations in growth of small crystals, *Phys. Rev. Lett*. 70:1143 (1993).
19. M. ELBAUM, S. G. LIPSON, and J. G. DASH, Optical study of surface melting on ice, *J. Cryst. Growth* 129:491 (1993).
20. M. MARUYAMA, N. KURIBAYASHI, K. KAWABATA, and J. S. WETTLAUFER, Shocks and curvature dynamics: A test of global kinetic faceting in crystals, *Phys. Rev. Lett*. 85:2545 (2000).
21. T. FUJIOKA and R. F. SEKERKA, Morphological stability of disc crystals, *J. Cryst. Growth* 24/25:84 (1974); H. MÜLLER-KRUMBHAAR, T. W. BURKHARDT, and D. M. KROLL, A generalized kinetic equation for crystal growth, *J. Cryst. Growth* 38:13 (1977); M. UWAHA, Asymptotic growth shapes developed from two-dimensional nuclei, *J. Cryst. Growth* 80:84 (1987); J. M. FLESSELLES, M. O. MAGNASCO, and A. J. LIBCHABER, From disks to hexagons and beyond: A study in two dimensions, *Phys. Rev. Lett*. 67:2489 (1991); B. B. BERGE, L. FAUCHEUX, K. SCHWAB, and A. J. LIBCHABER, Faceted crystal growth in two dimensions, *Nature* 350:322 (1991); J. TERSOFF, A. W. DENIER VAN DER GON, and R. M. TROMP, Critical island size for layer-by-layer growth, *Phys. Rev. Lett*. 72:266 (1994); T. MICHELY, M. HOHAGE, M. BOTT, and G. COMSA, Inversion of growth speed anisotropy in two dimensions, *Phys. Rev. Lett*. 70:3943 (1993); H. RÖDER, E. HAHN, H. BRUNE, J. P. BUCHER, and K. KERN, Building one- and two-dimensional nanostructures by diffusion-controlled aggregation at surfaces, *Nature* 366:141 (1993).
22. M. ADDA BEDIA and M. BEN AMAR, Faceting in free dendritic growth, *Phys. Rev. E* 51:1268 (1995).
23. A. J. BERNOFF and A. L. BERTOZZI, Singularities in a modified Kuramoto–Sivashinsky equation describing interface motion for phase transition, *Physica D* 85:375 (1995).

24. J. W. Cahn, J. E. Taylor, and C. A. Handwerker, Evolving crystal forms: Frank's characteristics revisited, in *Sir Charles Frank, OBE, FRS, An eightieth birthday tribute* (R. G. Chambers, J. E. Enderby, A. Keller, A. R. Lang, and J. W. Steeds, Eds.), pp. 88–118, Hilger, New York, 1991.
25. M. Gage and R. S. Hamilton, The heat-equation shrinking convex plane curves, *J. Diff. Geom*. 23:69 (1986).
26. R. LeVeque, private communication.
27. V. Tsemekhman and J. S. Wettlaufer, Shocks prevent continuous curvature divergence in interface motion, *Phys. Rev. Lett*. 87:205701 (2001).
28. M. Maruyama, private communication.
29. J. D. Weeks and G. H. Gilmer, Dynamics of crystal growth, *Adv. Chem. Phys*. 40:157 (1979).
30. J. Krug, M. Plischke, and M. Siegert, Surface diffusion currents and the university classes of growth, *Phys. Rev. Lett*. 70:3271 (1993).
31. E. D. Williams et al., Thermodynamics and statistical mechanics of the faceting of stepped Si(111), *Surf. Sci*. 294:219 (1993); A. Pimpinelli et al., Equilibrium step dynamics on vicinal surfaces, *Surf. Sci*. 295:143 (1993).
32. W. K. Burton, N. Cabrera, and F. C. Frank, The growth of crystals and the equilibrium structure of their surfaces, *Phil. Trans. R. Soc. A* 243:299 (1951).
33. V. Tsemekhman and J. S. Wettlaufer, Shocking facets in interface growth, *J. Cryst. Growth* 235:589 (2002).

University of Washington
Yale University

(Received April 24, 2002)